2014-10

A Crystalline Oxide Passivation for Al_2O_3/AlGaN/GaN

UTD AUTHOR(S): Xiaoye Qin, Hong Dong, Jiyoung Kim and Robert M. Wallace

Qin, X., H. Dong, J. Kim, and R. M. Wallace. 2014. "A crystalline oxide passivation for Al_2O_3/AlGaN/GaN." Applied Physics Letters 105(14): 141604-1 to 5.

A crystalline oxide passivation for Al2O3/AlGaN/GaN

Xiaoye Qin, Hong Dong, Jiyoung Kim, and Robert M. Wallace

Citation: Applied Physics Letters **105**, 141604 (2014); doi: 10.1063/1.4897641
View online: http://dx.doi.org/10.1063/1.4897641
View Table of Contents: http://scitation.aip.org/content/aip/journal/apl/105/14?ver=pdfcov
Published by the AIP Publishing

A crystalline oxide passivation for Al_2O_3/AlGaN/GaN

Xiaoye Qin, Hong Dong, Jiyoung Kim, and Robert M. Wallace[a)]
Department of Materials Science and Engineering, The University of Texas at Dallas, Richardson, Texas 75080, USA

(Received 8 July 2014; accepted 29 September 2014; published online 9 October 2014)

In situ X-ray photoelectron spectroscopy and low energy electron diffraction are performed to study the formation of a crystalline oxide on the AlGaN surface. The oxidation of the AlGaN surface is prepared by annealing and remote $N_2 + O_2$ plasma pretreatments resulting in a stable crystalline oxide. The impact of the oxide on the interface state density is studied by capacitance voltage (C-V) measurements. It is found that a remote plasma exposure at 550 °C shows the smallest frequency dispersion. Crystalline oxide formation may provide a novel passivation method for high quality AlGaN/GaN devices. © *2014 AIP Publishing LLC*.
[http://dx.doi.org/10.1063/1.4897641]

Nitride-based AlGaN/GaN high electron mobility transistors (HEMTs) are ideal for high-frequency, high power, and high temperature devices.[1] However, a large leakage current is a key limitation in device applications.[2] To address this issue, a typical method entails the insertion of an insulator (typically oxides such as Al_2O_3 and HfO_2) layer between the gate metal and AlGaN, producing a MOSHEMT structure.[3,4] An Al_2O_3 amorphous dielectric layer, deposited by atomic layer deposition (ALD), is often employed for gate isolation in III-V transistors due to (i) the large band gap (8.7 eV), (ii) high breakdown field (10 MV/cm), (iii) a relatively high dielectric constant ($k \sim 10$), and (iv) the reduction of native oxides by the ALD process as well as a barrier to subsequent surface reoxidation resulting in interfacial bonding disorder.[5,6] The ALD of Al_2O_3 also offers well controlled growth rates and high aspect ratio conformal growth. However, the quality of the Al_2O_3/AlGaN interface remains a challenge.[7–9] In contrast, Miao *et al.*[10] recently proposed the possibility of an energetically favorable 2 monolayer (ML) crystalline oxide structure obeying the electron counting rule (2 ML EC)[11] on GaN and AlN using first-principles simulations. In that work, it was noted that the "2 ML EC" structure was likely to form under realistic oxidation conditions and has a relatively low density of surface states within the band gap. Moreover, partially ordered oxide structures have been reported to form on GaN upon O_2 exposure at 550 °C.[12] However, the impact of oxidation of AlGaN on device performance is still under much debate with apparently contrasting experimental outcomes.[13,14] Additionally, the prospect of a high quality interfacial passivation layer, stable to high-k ALD processes, may enable improve MOSHEMT performance.

To examine this possibility, we employ *in situ* monochromatic X-ray photoelectron spectroscopy (XPS) and low energy electron diffraction (LEED) characterization to study the interfacial chemistry and structure of the oxidation of AlGaN by annealing and remote $N_2 + O_2$ plasma treatments. A stable crystalline oxide layer, ~2 ML thick, is detected on the AlGaN surface pretreated by the remote plasma at 550 °C. Unlike the case for III-arsenides,[15] the ordered oxide appears to persist upon subsequent exposure to aggressive ALD precursors at 300 °C. Frequency dependent C-V measurements confirm that the crystalline oxide layer reduces the interface state density for ALD-Al_2O_3 on AlGaN significantly.

Metal organic chemical vapor deposited $Al_{0.25}Ga_{0.75}N$ (30 nm)/GaN (1.2 μm) layer on a p-type Si(111) substrate HEMTs wafers obtained from DOWA Electronics Materials (Tokyo, Japan) were used in this study. The AlGaN orientation was (0001). Four samples ($\sim 1 \times 1\,cm^2$) from the same wafer were first solvent cleaned in acetone, methanol, and isopropanol for 1 min each to reduce surface organic contamination and then introduced to an ultra-high vacuum (UHV) cluster system described in detail elsewhere.[15] Sample "A" consisted of a native oxide AlGaN/GaN/Si control sample. Sample "B" was exposed to a N_2:O_2 anneal (45 sccm $N_2 + 0.5$ sccm O_2) at 550 °C for 10 min in a connected UHV preparation chamber. Samples "C" and "D" were exposed to a N_2:O_2 remote plasma (45 sccm $N_2 + 0.5$ sccm O_2) at 300 °C and 550 °C for 10 min, respectively, in the same preparation chamber. After these pretreatments, *in situ* XPS and LEED were performed on all samples. Then, the samples were transferred to a Picosun ALD reactor through a transfer tube (operating pressure: 1×10^{-10} mbar) to avoid spurious atmospheric contamination followed by exposure to one pulse of Tri-methyl Aluminum (TMA). Then, *in situ* XPS and LEED were again performed for on all samples after they were similarly transferred to analysis chamber. After subsequent exposure to 20 and 80 full ALD cycles (total 100 cycles) of Al_2O_3, XPS was performed again to monitor the chemical changes at interfaces. All ALD was performed using TMA and H_2O as precursors. One full ALD cycle was 0.1 s TMA + 4 s purge + 0.1 s H_2O + 4 s purge. High purity (99.999%) N_2 (200 sccm) was used as the precursor carrier and purging gas. The working pressure of the ALD reactor was ~10 mbar and the Al_2O_3 deposition temperature was 300 °C.

After the total of 100 cycles (~10 nm) of ALD Al_2O_3, the samples were taken out of the deposition and analysis system for diode fabrication. Ohmic contact regions were defined first by standard photolithography and contact regions to the AlGaN layer were opened by 20 s BCl_3

[a)]Electronic mail: rmwallace@utdallas.edu

(15 sccm)/Ar (5 sccm) reactive ion etching (RIE). It was verified that the RIE removed the ~10 nm Al_2O_3 and ~2 nm AlGaN by *ex situ* ellipsometry and XPS. The ohmic contacts (resistivity $\rho \sim 1 \times 10^{-6}$ Ω cm^2) were formed by e-beam evaporation deposition (base pressure $\sim 1 \times 10^{-6}$ mbar) of Ti/Al/Ni/Au (20 nm/100 nm/50 nm/50 nm) followed by rapid thermal annealing at 850 °C for 30 s with 2000 sccm N_2 after patterning by lift off.[16] Circular gate electrodes were then defined, followed by e-beam deposition of Ni/Au (50 nm/100 nm) and lift off. C-V measurements were performed by an Agilent 4284 LCR meter with step of 0.02 V and AC modulation voltage of 50 mV with sweep frequencies varying from 5 to 400 kHz.

XPS was carried out using a monochromated Al Kα_1 ($h\nu = 1486.7$ eV) X-ray source, equipped with a 7 channel analyzer, using a pass energy of 15 eV, with all scans taken at 45° with respect to the sample normal. XPS peak deconvolution was accomplished using a Analyzer software with a detailed peak fitting procedure described elsewhere.[17] All peaks were referenced to the N 1*s* peak at 397.0 eV to compensate for any changes in the peak core level positions due to band bending.

Fig. 1 shows *in situ* N 1*s* and Ga *LMM* Auger spectra for samples A, B, C, and D. The spectra for sample A are shown for reference with the N-Ga/Al N1*s* peaks (set at 397.0 eV), and the Ga $L_2M_{45}M_{45}$ Auger feature (spanning ~ 392–398 eV).[18] As shown in Fig. 1(a), the N 1*s* and Ga *LMM* spectra for the samples A and B overlap fully, clearly showing that the 550 °C annealing pretreatment in the 45 sccm $N_2 + 0.5$ sccm O_2 flow does not change the chemical state of nitrogen or the Ga/N ratio (Ga *LMM* area/N 1*s* area). However, an obvious peak at 402 eV, corresponding to N-O bonding for sample B,[19] is detected (Fig. 1(b)). The detection of N-O bonding indicates that the oxidation layer generated by the 300 °C plasma does not conform to the proposed "2 ML EC" structure that does not formally contain N-O bonds,[10] as seen in Fig. 1(e). Apart from the N-O bonding, a feature at 398 eV is also detected, which

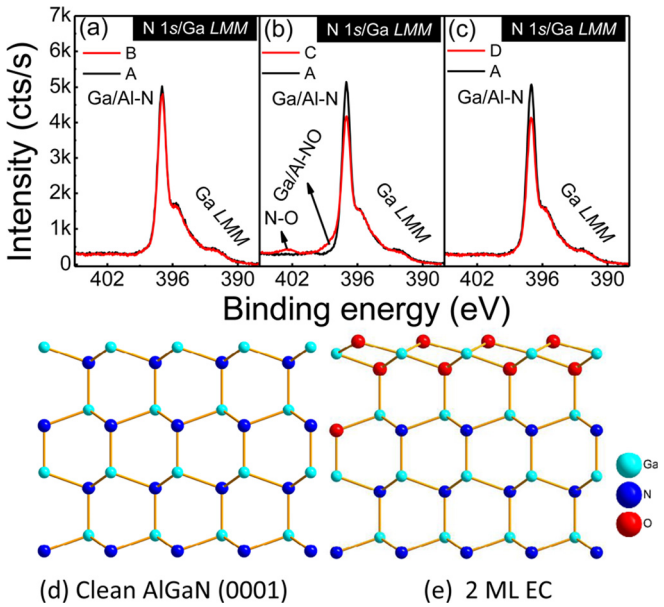

FIG. 1. *In situ* XPS spectra of the N 1*s* and Ga *LMM* for samples A, B, C, and D. Schematic of the side view of (d) clean and (e) 2 ML EC AlGaN (0001) structures.

likely originates from Ga/Al-ON[20] and N-C(H).[21] However, since the C 1*s* intensity for sample C is near the XPS detection limits (see Fig. S1 in the supplementary material[22]) and the intensity of N-C(H) is very low according to our previous study for *in situ* N_2 and forming gas plasma pretreatments on AlGaN.[21] This observation leads to the conclusion that the feature mainly originates from Ga/Al-ON bonding. In contrast, there is no evidence of N-O or Ga/Al-O-N feature detected for sample D (Fig. 1(c)), which is in agreement with the proposed "2 ML EC" model.[10] These results indicate that the 550 °C is likely able to oxidize the AlGaN surface to saturation, similar to that reported previously for GaN.[12] It is noted that the Ga/Al-N peak intensity for samples C and D (Figs. 1(b) and 1(c)) is lower than that for sample A, but the Ga *LMM* Auger feature intensity remains constant for all samples, indicating that the N intensity is attenuated by the oxide/oxynitride present on the surface of samples C and D, which will be discussed further below.

Fig. 2 shows that the *in situ* normalized Ga $2p_{3/2}$ and Al 2*p* spectra for samples A, B, C, and D. Consistent with our prior work,[21,23,24] the Ga $2p_{3/2}$ spectra from sample A show two peaks, indicative of Ga-N (at 1117.8 eV) from the AlGaN substrate and the presence of a Ga^{3+} oxidation state (1118.5 eV) from the surface. Additionally, the Al 2*p* spectra for sample A also show two peaks consistent with Al-N bonding (at 73.5 eV) and Al-O bonding (at 74.4 eV). It is noted that the "2 ML EC" model of the oxidation layer of GaN/AlN consists of Ga-O/Al-O, while Ga-Ga/Al-Al or Ga/Al-ON bonds should not be detected in the structure.[10] The same spectral fitting parameters are used as in previous work[21,23,24] and the ratios of Ga-O(N)/Ga-N and Al-O(N)/Al-N are shown in Table I. The estimated error of ratio is based on the fitting procedure.[21,23] The 550 °C annealing pretreatment results in a slight increase of the Ga-O and Al-O concentrations (Table I). Larger Ga-O and Al-O concentrations are detected from samples C and D compared to B due to the remote plasma exposure, while the 550 °C plasma pretreatment does not contribute to additional oxide formation than the 300 °C remote plasma pretreatment.

Although the Ga/Al-ON state is clearly detected from the N 1*s* spectra for sample C, it is complicated to deconvolve the Ga/Al-ON from Ga $2p_{3/2}$/Al 2*p* due to ambiguous Ga-ON peak parameters (such as the associated binding

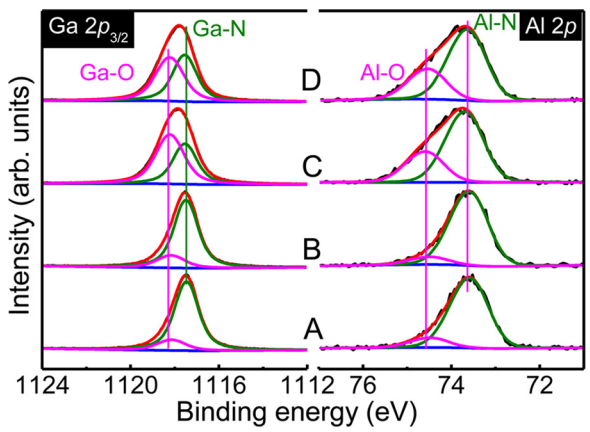

FIG. 2. *In situ* XPS spectra of the normalized Ga $2p_{3/2}$ and Al 2*p* for samples A, B, C, and D.

TABLE I. Summary of sample pretreatments, rations of Ga-O(N)/Ga-N and Al-O(N)/ Al-N, observed threshold voltage.

Samples	Pretreatments	Ga-O(N)/Ga-N	Al-O(N) Al-N	V_{TH} (V)	D_{it} ($cm^{-2}eV^{-1}$) ($0.34 < E_C - E_T < 0.45$ eV)
A	Native	0.17 ± 0.01	0.10 ± 0.006	−9.4	2.00×10^{14}
B	550 °C $N_2 + O_2$ anneal	0.19 ± 0.01	0.11 ± 0.006	−11	2.79×10^{14}
C	300 °C $N_2 + O_2$ plasma	0.99 ± 0.09	0.44 ± 0.01	−8.6	3.27×10^{14}
D	550 °C $N_2 + O_2$ plasma	0.84 ± 0.08	0.42 ± 0.01	−5.6	3.81×10^{13}

energy[25]). Therefore, the fitting for sample C is still based on the two peaks for a consistent fit in this work. The concentration of Ga-ON could be evaluated simply by the intensity of Ga-ON in N 1*s* in Fig. 1(b). Assuming that Ga-ON contributes entirely to the peak at 398 eV (Fig. 1(b)), the concentration of Ga-ON is ∼17% of the oxide/oxynitride on sample C. From XPS thickness calculations, based on the attenuation of N 1*s* spectra in Figs. 1(b) and 1(c), a ∼0.3 nm oxide layer for samples C and D is detected, indicating that almost 1 ML of nitrogen on samples C and D is replaced by oxygen from the remote plasma process and 2 ML of oxide is formed which is consistent with the "2 ML EC" structure,[10] as seen in Figs. 1(d) and 1(e). Further discussions on the C 1*s* and O 1*s* spectra are shown in the supplementary materials.[22]

The LEED characterization, which is sensitive to the surface atomic order, is performed to evaluate the surface structure for samples A, B, C, and D. Fig. 3(a) shows the LEED pattern for the sample A as reference, which shows a sharp (1×1) hexagonal pattern indicative of the AlGaN surface, albeit with a 0.8 ± 0.2 ML nonuniform physisorbed carbon contamination layer. The (1×1) pattern is consistent with LEED patterns from as exfoliated MoS_2 (Ref. 26) as a reference sample, and details are included in the supplementary materials,[22] indicating an unreconstructed (1×1) structure. The carbon coverage is calculated from XPS intensity.[21] Fig. 3(b) also shows the same hexagonal pattern as the sample A, indicating that the annealing pretreatment does not change the surface structure. It should be noted that samples A and B do not correspond to the clean surface shown in Fig. 1(a). However, the oxygen on the surfaces of samples A or B, which is less than 1 ML,[23] does not change the (1×1) surface structure. This is also observed by Bermudez by comparison of clean and O_2 exposed surfaces.[27] The possible adsorption site for oxygen on the surface is at the "on top" or fcc position.[28] However, a LEED pattern in Fig. 3(c) for sample C does not show any ordered structure, suggesting that the 300 °C plasma pretreatment produces an amorphous oxide/oxynitride layer. Considering the presence of the Ga-ON and N-O bonding in Fig. 1(b), the surface is likely disordered as a result of the incomplete oxidation at the 300 °C plasma pretreatment. In contrast, a sharp hexagonal pattern for sample D is observed in Fig. 3(d), which is the direct evidence of ordered oxide layer. Thus, the formation of the crystalline oxide is temperature dependent. Dong *et al.*[12] also reported the same temperature dependent phenomenon for the *in situ* oxidization of GaN by molecular oxygen. However, it should be noted that the LEED pattern observed by Dong *et al.* corresponds to a $(3\sqrt{3} \times 3\sqrt{3}\text{-R30}^\circ)$ reconstruction and is likely due to the existence of a Ga bilayer on the starting surface.[12] To summarize, the oxidation of AlGaN can be achieved by 300 °C and 550 °C plasma pretreatments, while the 550 °C plasma pretreatment contributes to an order crystalline oxides exhibiting a (1×1) LEED pattern which is consistent with the proposed "2 ML EC" surface oxide structure proposed by Miao *et al.*,[10] which is expected to reduce the interface state density (D_{it}).

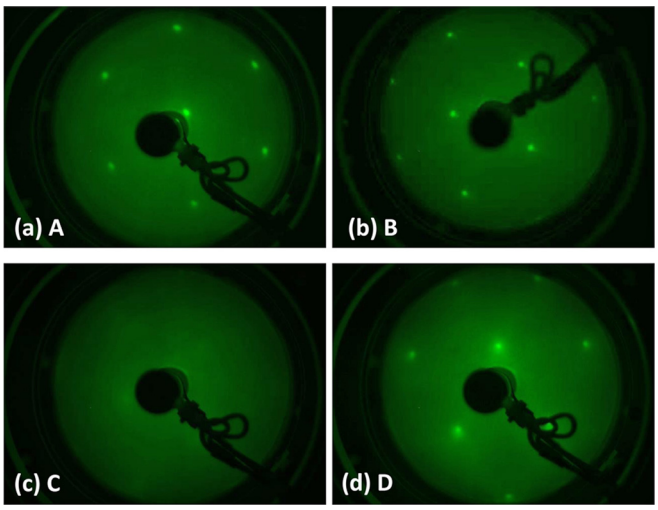

FIG. 3. LEED patterns for samples A, B, C, and D taken with an electron beam energy of 113 eV.

Punkkinen *et al.*[29] recently proposed that an ordered, well-defined crystalline oxide layer on InAs has the potential to provide defect-free interface enabling a new method for metal oxide semiconductor field-effect transistors (MOSFETs) and tunnel field-effect transistors (TFETs) applications. The stability of that crystalline oxide layer on InAs(100), prepared by *in situ* thermal anneal in O_2 atmosphere, upon exposure to ALD has also been investigated with *in situ* XPS and LEED.[30] Although the oxidation process produces an ordered (3×1)-O reconstruction on InAs, this oxide layer could be reduced easily by even one pulse of TMA due to the "clean-up effect." In contrast, the crystalline oxide on sample D is stable upon such ALD exposures, and is discussed further in the supplementary materials.[22]

In order to evaluate the D_{it} of Al_2O_3/AlGaN/GaN interface for these pretreatments, the corresponding Al_2O_3 (∼10 nm)/AlGaN/GaN diodes were fabricated.[7,8,31] Figure 4 shows the C-V curves with the measurement frequency varied from 5 kHz to 400 kHz at room temperature for samples A, B, C, and D, and the details of the C-V response in such

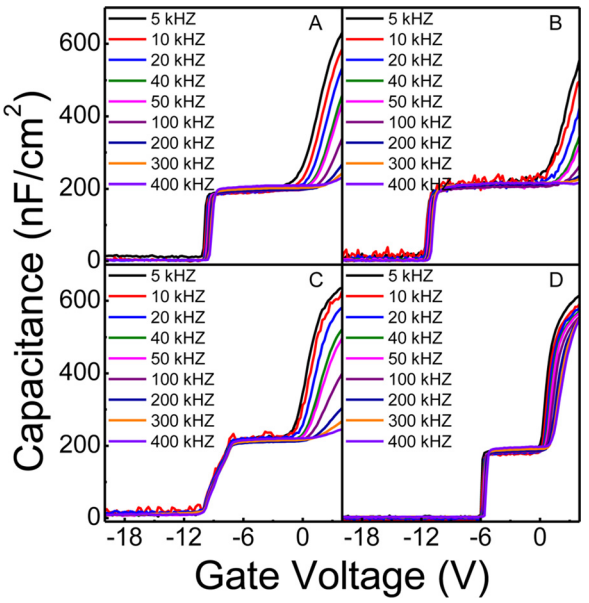

FIG. 4. Frequency-dependent C-V curves from capacitors for samples A, B, C, and D.

device structures have been reported.[7,8,31–34] The frequency dispersion originating from the Al_2O_3/AlGaN interface traps response is visible in the second slope region ($V_{gate} > -3$ V) for the sample A. The 550 °C annealing pretreatment does not reduce the dispersion and the 300 °C remote plasma exposure results in even worse frequency dispersion due to the amorphous oxide/oxynitride layer. The gradual C-V slope for the first step ($V_{gate} \sim -11$ V) from sample C indicates the high D_{it} as a result of low quality of oxide/oxynitride layer again.[4] In contrast, the smallest amount of frequency dispersion is detected from the sample D, suggesting that the oxide layer on the sample D reduces the interface state density substantially.

The resulting benefits of the crystalline oxide interlayer are substantial. First, the crystalline oxide saturates the Ga/Al dangling bonds for the Ga/Al-terminated AlGaN surface. The interfacial bonding between AlGaN and Al_2O_3 is one possible reason of high D_{it}.[35] The high quality of a crystalline oxide as a passivation layer between AlGaN and Al_2O_3 reduces the D_{it}. The observed threshold voltage (V_{TH}) values from the curves measured at 100 kHz for samples A, B, C, and D in Fig. 4 are shown in Table I. It should be noted that the gradual/gentle C-V slope for sample makes the error of V_{TH} relatively high ($\sim \pm 1.5$ V). In particular, the crystalline oxide results in a 3.8 V positive shift. We speculate that the high fixed positive charge density at ALD-Al_2O_3/AlGaN[36] is reduced by the crystalline oxide passivation layer. In contrast, the positive V_{TH} shift effect is not obvious for samples B and C. This crystalline passivation layer also provides a potential for fabricating low D_{it} normally off Al_2O_3/AlGaN/GaN MOSHEMTs (Table I). The extraction of D_{it} ($0.34 < E_C - E_T < 0.45$ eV) refers to the method presented in Ref. 33.

In conclusion, the oxidation behavior of AlGaN is investigated by *in situ* XPS and LEED and *ex situ* C-V characterization. Oxidation layers 2 ML could be achieved by 300 °C and 550 °C $N_2 + O_2$ plasma pretreatments. In particular, the 550 °C remote plasma pretreatment contributes to a stable crystalline oxide layer and inhibits the formation of N-O and Ga-ON bonds, which likely contribute to interface defects. Additionally, AlGaN/GaN MOS diodes pretreated by the 550 °C plasma exhibit a good interface quality with the smallest frequency dispersion indicating a lower D_{it}. This crystalline oxide passivation will have potential for high quality of AlGaN/GaN MOSHEMTs.

The authors thank Mr. Greg Mordi and Mr. Antonio Lucero for helpful discussions. This work was supported by the Asian Office of Aerospace Research and Development (AOARD) through the Air Force office of Scientific Research (AFOSR) under Grant No. FA2384-11-1-0477. J. Kim also acknowledges financial support by the IT R&D program of MOTIE/KETI (Grant No. 10048933).

[1]U. K. Mishra, P. Parikh, and Y. F. Wu, Proc. IEEE **90**, 1022 (2002).
[2]J. W. Chung, J. C. Roberts, E. L. Piner, and T. Palacios, IEEE Electron Device Lett. **29**, 1196 (2008).
[3]M. A. Khan, X. Hu, A. Tarakji, G. Simin, J. Yang, R. Gaska, and M. S. Shur, Appl. Phys. Lett. **77**, 1339 (2000).
[4]T. Hashizume, S. Ootomo, T. Inagaki, and H. Hasegawa, J. Vac. Sci. Technol. B **21**, 1828 (2003).
[5]S. McDonnell, H. Dong, J. M. Hawkins, B. Brennan, M. Milojevic, F. S. Aguirre-Tostado, D. M. Zhernokletov, C. L. Hinkle, J. Kim, and R. M. Wallace, Appl. Phys. Lett. **100**, 141606 (2012).
[6]G. D. Wilk, R. M. Wallace, and J. M. Anthony, J. Appl. Phys. **89**, 5243 (2001).
[7]S. Huang, S. Yang, J. Roberts, and K. J. Chen, Jpn. J. Appl. Phys., Part 1 **50**, 110202 (2011).
[8]C. Mizue, Y. Hori, M. Miczek, and T. Hashizume, Jpn. J. Appl. Phys., Part 1 **50**, 021001 (2011).
[9]T. Hung, M. Esposto, D. N. Nath, S. Krishnamoorthy, P. S. Park, and S. Rajan, in *International Conference on Compound Semiconductor Manufacturing Technology* (2013), pp. 191–194.
[10]M. S. Miao, J. R. Weber, and C. G. Van de Walle, J. Appl. Phys. **107**, 123713 (2010).
[11]M. Pashley, Phys. Rev. B **40**, 10481 (1989).
[12]Y. Dong, R. M. Feenstra, and J. E. Northrup, J. Vac. Sci. Technol. B **24**, 2080 (2006).
[13]O. I. Saadat, J. W. Chung, E. L. Piner, and T. Palacios, IEEE Electron Device Lett. **30**, 1254 (2009).
[14]M. Tajima, J. Kotani, and T. Hashizume, Jpn. J. Appl. Phys., Part 1 **48**, 020203 (2009).
[15]R. M. Wallace, ECS Trans. **16**, 255 (2008).
[16]S. Ruvimov, Z. Liliental-Weber, J. Washburn, K. J. Duxstad, E. E. Haller, Z.-F. Fan, S. N. Mohammad, W. Kim, A. E. Botchkarev, and H. Morkoç, Appl. Phys. Lett. **69**, 1556 (1996).
[17]B. Brennan and G. Hughes, J. Appl. Phys. **108**, 053516 (2010).
[18]E. Antonides, E. C. Janse, and G. A. Sawatzky, Phys. Rev. B **15**, 1669 (1977).
[19]G. V. Soares, K. P. Bastos, R. P. Pezzi, L. Miotti, C. Driemeier, I. J. R. Baumvol, C. Hinkle, and G. Lucovsky, Appl. Phys. Lett. **84**, 4992 (2004).
[20]Z. L. Fang, J. Y. Kang, and W. Z. Shen, J. Phys. Chem. C **112**, 17652 (2008).
[21]X. Qin, H. Dong, B. Brennan, A. Azacatl, J. Kim, and R. M. Wallace, Appl. Phys. Lett. **103**, 221604 (2013).
[22]See Supplemental Material at http://dx.doi.org/10.1063/1.4897641 for additional XPS and LEED results.
[23]X. Qin, B. Brennan, H. Dong, J. Kim, C. L. Hinkle, and R. M. Wallace, J. Appl. Phys. **113**, 244102 (2013).
[24]B. Brennan, X. Qin, H. Dong, J. Kim, and R. M. Wallace, Appl. Phys. Lett. **101**, 211604 (2012).
[25]Z. L. Fang, J. Y. Kang, and W. Z. Shen, Nanotechnology **20**, 045401 (2009).
[26]A. Azcatl, S. McDonnell, S. K. C., X. Peng, H. Dong, X. Qin, R. Addou, G. I. Mordi, N. Lu, J. Kim, M. J. Kim, K. Cho, and R. M. Wallace, Appl. Phys. Lett. **104**, 111601 (2014).
[27]V. M. Bermudez, J. Appl. Phys. **80**, 1190 (1996).
[28]T. K. Zywietz, J. Neugebauer, and M. Scheffler, Appl. Phys. Lett. **74**, 1695 (1999).

[29]M. P. J. Punkkinen, P. Laukkanen, J. Lång, M. Kuzmin, M. Tuominen, V. Tuominen, J. Dahl, M. Pessa, M. Guina, K. Kokko, J. Sadowski, B. Johansson, I. J. Väyrynen, and L. Vitos, Phys. Rev. B **83**, 195329 (2011).
[30]D. M. Zhernokletov, P. Laukkanen, H. Dong, R. V. Galatage, B. Brennan, M. Yakimov, V. Tokranov, J. Kim, S. Oktyabrsky, and R. M. Wallace, Appl. Phys. Lett. **102**, 211601 (2013).
[31]X. Qin, A. Lucero, A. Azcatl, J. Kim, and R. M. Wallace, Appl. Phys. Lett. **105**, 011602 (2014).
[32]S. Yang, Z. Tang, K. Wong, Y. Lin, C. Liu, Y. Lu, S. Huang, and K. J. Chen, IEEE Electron Device Lett. **34**, 1497 (2013).
[33]D. W. Johnson, R. T. P. Lee, R. J. W. Hill, M. H. Wong, G. Bersuker, E. L. Piner, P. D. Kirsch, and H. R. Harris, IEEE Trans. Electron Devices **60**, 3197 (2013).
[34]M. Fagerlind, F. Allerstam, E. Ö. Sveinbjörnsson, N. Rorsman, A. Kakanakova-Georgieva, A. Lundskog, U. Forsberg, and E. Janzén, J. Appl. Phys. **108**, 014508 (2010).
[35]X. Wang, L. Dong, J. Zhang, Y. Liu, P. D. Ye, and R. G. Gordon, Nano Lett. **13**, 594 (2013).
[36]J. Son, V. Chobpattana, B. M. McSkimming, and S. Stemmer, Appl. Phys. Lett. **101**, 102905 (2012).